International Journal of Heat and Mass Transfer 97 (2016) 861–867

Contents lists available at ScienceDirect

International Journal of Heat and Mass Transfer

journal homepage: www.elsevier.com/locate/ijhmt

Microscopic observation of frost behaviors at the early stage of frost formation on hydrophobic surfaces

Hisuk Kim, Donghee Kim, Hanmin Jang, Dong Rip Kim, Kwan-Soo Lee *

School of Mechanical Engineering, Hanyang University, Wangsimni-ro 220, Seoul 133-791, South Korea

ARTICLE INFO

Article history:
Received 21 August 2015
Received in revised form 2 February 2016
Accepted 2 February 2016
Available online 14 March 2016

Keywords:
Frost formation
Hydrophobic
Surface treatment
Frost retardation
Early stage of frost

ABSTRACT

Microscopic seed behavior in the early stage of frost formation was experimentally observed with different fin surface contact angles from bare to superhydrophobicity under air-source heat pump operating conditions. The seed average height, radius, number, and frost density at the early stage of frost were analyzed. As the surface contact angle increased, the seed average height and number increased, while the seed radius and frost density decreased. A correlation with a Fourier number was proposed from the measured data. With the correlation, the large and small frost retardation effect regions were identified.

1. Introduction

Heat exchangers are widely used under frosting conditions, in air-source heat pumps (ASHPs) and heating, ventilation, and air conditioning (HVAC) systems of electric vehicles. When frost develops, the heat resistance increases and the air path becomes blocked; thus, the thermal performance of heat exchangers and the corresponding total system efficiencies significantly decrease. To overcome this issue, the fin surface of the heat exchanger was rendered hydrophobic or superhydrophobic, thereby retarding the frosting phenomenon. These surface treatments can delay the freezing time by increasing the seed formation period.

A surface-treated heat exchanger has many benefits over untreated one [1–3]. A hydrophobic heat exchanger exhibits better thermal performance. Kim and Lee [1–3] compared surface-treated heat exchangers; they found that the hydrophobic heat exchanger had better thermal performance under frosting conditions than the bare one. However, most research conducted to date has been from a macroscopic point of view, and these authors only verified the effects of frost retardation of heat exchanger, not the microscopic phenomena.

Considerable research has focused on hydrophobic or superhydrophobic surface treatments for frosting retardation. He et al. [4] made hydrophobic (98.1°) and superhydrophobic (155.3°) samples using i-PP (isotactic polypropylene) film and conducted frost retardation experiments. He et al. [5] also carried out the frost retardation experiments on superhydrophobic (154.6–170.9°) samples. Jung et al. [6] studied frost retardation at −20 °C cold plate temperature using 90–150° samples. Inada et al. [7] reported that frost retardation was effective on hydrophobic surfaces through supercooling by decreasing the surface temperature 0.07 °C per second, −20 °C to −45 °C, using a variety of water contact angle samples. Other researchers have reported the fabrication of hydrophobic or superhydrophobic samples using various methods of surface treatment to realize the notable frost retardation effects [8–14]. However, those studies focused on the development of materials for making superhydrophobic surfaces or conducted the experiments of single droplets on a surface to investigate supercooling, so their findings are not sufficient to explain the effects of frost retardation in real applications.

In order to understand how the surface treatment affect the frosting retardation phenomena in real applications, we observed and analyzed microscopic seed behavior at early stages of frost formation under heat pump operating conditions. Specifically, we investigated the seed height, radius, number, and frost density, in the early stages of frost under various operating conditions using a novel experimental method suggested in previous research [15]. Through microscopic observation, we examined how the surface treatments retard frosting. Additionally, we propose the operating condition region, where surface treatments are effective to realize the frost retardation using a Fourier number.

* Corresponding author.
E-mail address: ksleehy@hanyang.ac.kr (K.-S. Lee).

http://dx.doi.org/10.1016/j.ijheatmasstransfer.2016.02.020
0017-9310/

Nomenclature

a	distance from the origin in Eq. (2) [m]
b	distance from the origin in Eq. (7) [m]
h	height [m]
Fo	Fourier number [–]
L	specimen length [m]
m_w	absolute humidity [kg/kg$_{DA}$]
N	number of seeds [#]
r	radius [m]
Re	Reynolds number [–]
t	time [min]
T	temperature [°C]
u	velocity [m/s]
V	volume [m^3]
x, y	x, y coordinates [–]

Greek symbols

α	thermal diffusivity [m^2/s]
v	kinematic viscosity [m^2/s]
ρ	frost density [kg/m^3]
θ	water contact angle [°]

Subscripts

a	air
avg	average
eff	effective
f	frost
r	refrigerant
total	total
tp	triple point

2. Experimental methodology

2.1. Experimental setup and test conditions

Fig. 1 shows the test section ($L \times W \times H$ = 500 × 300 × 300 mm) of the experimental setup. The experimental apparatus was configured in the same manner as in previous studies [15–17], but the test section was modified. As shown in Fig. 1, two high-resolution cameras which were installed at the top and side captured the seed patterns, such as, radius, height, and distribution. Additionally, we accurately measured the freezing time when seeds changed from water to ice by installing a luminance meter on the top of the test section. Samples used in this study were similar to a previous study; six samples from bare to a water contact angle of 160°.

Test conditions (Table 1) were selected based on ASHP extreme operating conditions, (8 °C/6 °C), as mentioned in the ANSI/AHRI standard [18]. We constructed a four factors × three levels experimental design using four operating factors: refrigerant temperature, air temperature, air velocity, and relative humidity. Based on the CCF (face central composite design method), 25 different operating conditions were listed in Table 2. From CCF, we defined the three representative operating conditions: (1) the low condition (refrigerant temperature −14 °C, air temperature 4 °C, air velocity 2 m/s, relative humidity 60%, #1), (2) the reference condition (refrigerant temperature −11 °C, air temperature 6 °C, air velocity 3 m/s, relative humidity 75%, #25), and (3) the high condition (refrigerant temperature −8 °C, air temperature 8 °C, air velocity 4 m/s, relative humidity 75%, #16). For each operating condition, the experiments were conducted with the samples of six different surface contact angles.

2.2. Data measurements

The top camera captured the seed distribution and radius, while the side camera captured the seed height. Using NIS-Elements Documentation (NIS-Element D), we measured the seed average radius, the seed distribution on the sample, and the seed average height. The seed radius was measured at five different areas on the sample, and for each area the maximum radii of 10 seeds were measured. In total, the radii of 50 seeds were averaged. The seeds on the sample were very small and irregularly distributed. Therefore, to obtain the total number of seeds on the sample, the number density of the seeds per unit area were calculated by counting the number of the seeds in five different areas (0.1 × 0.1 cm), and then multiplied by the total sample area (5 × 5 cm). The seed height was averaged by measuring at the leading edge (1 cm), middle (1 cm), and the rear (1 cm) of the sample. The radius measured from the top view was compared with the calculated radius by using the frost height measured from the side view, and consequently, those were well matched each other within 5% error, thereby confirming that our measurement was not overestimated.

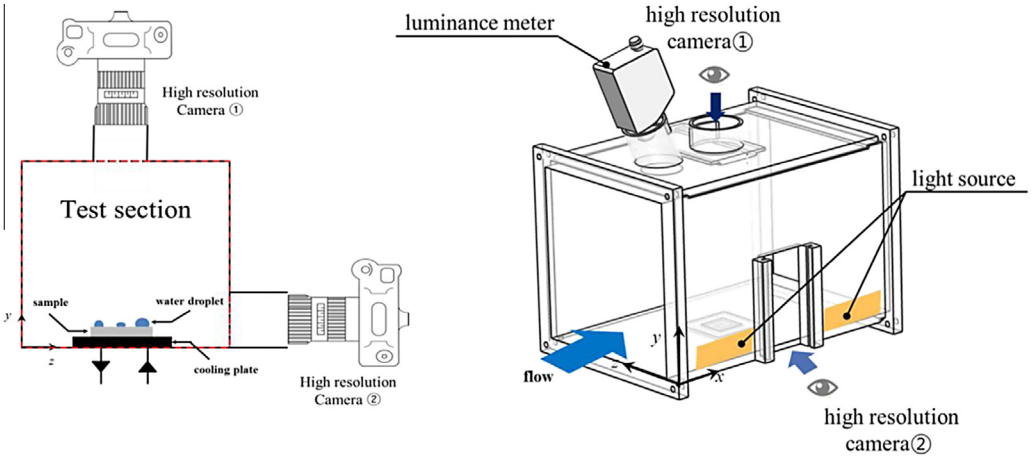

Fig. 1. Experimental apparatus for the tests.